

Fuzzy Logic Aided PID Controller for Induction Motor Speed Control

Cosmas Anayo Okeke

Department of Electrical and Electronic Engineering, Chukwuemeka Odumegwu Ojukwu University, Uli, Nigeria
Email: acofrancee@gmail.com

Innocent Ifeanyi Okonkwo

Department of Electrical and Electronic Engineering, Chukwuemeka Odumegwu Ojukwu University, Uli, Nigeria
Email: fins212@gmail.com

ABSTRACT

This paper presents design of intelligent based controller for speed control of induction motor. The proposed system integrates a classical proportional-integral-derivative (PID) controller and intelligent algorithm based on fuzzy logic control (FLC). This scheme takes advantages of classical PID and FLC to improve the speed response performance of induction motor analysed in terms of transient and steady state time domain characteristics. The FLC designed was implemented using the fuzzy block of MATLAB/Simulink based on Mamdani model and comprises 9 fuzzy variables and 49 logic (intelligent) rules that define the system behaviour. The FLC takes the loop error and its rate of change to manipulate the input command to the PID control so that the response speed signal matches with the desired speed signal resulting in reduced rise time, peak time, settling time, overshoot, and improved steady state error. The designed intelligent aided PID controller was implemented and the simulation result provided a rise time of 0.8354 second, peak time of 4.9615 seconds, settling time of 1.2240 seconds, final value (actual speed) of 1724.9 rpm, steady state error 0.1 rpm. Simulation comparison with conventional PID controller showed that the PID yielded a rise time of 1.6723 seconds, peak time of 4.5475 seconds, peak overshoot of 0.6913 %, settling time of 2.9646 seconds, final value (actual speed) 1736.1 rpm, and steady state error of 11.1 rpm. Generally, simulation results indicated that the intelligent (FLC) aided classical PID control improve the system performance and achieved the rated speed of the motor.

Keywords – Controller, Fuzzy logic, Induction motor, Speed control, PID

Date of Submission:

Date of Acceptance:

I. INTRODUCTION

The industrial application of induction motors is very vast. Induction motors are used in paper and textile mills, hybrid vehicles, wind generation systems, and robotics due to their many inherent benefits such as easy construction, reliability, robustness, low cost, and ease of maintenance [1]. It is virtually not possible for an induction motor to meet the desired function for any application industry without being properly controlled [2].

Many control schemes such as scalar control, direct torque control, and vector or field oriented control have been proposed to control induction motor so as to achieve maximum performance efficiency. One of the first control methods employed in induction motors is scalar control. This method of control involves keeping the ratio of the supply voltage amplitude and its frequency constant (commonly called v/f technique) so that a given air gap flux is maintained and thereby providing maximum torque. Drives employing scalar control are easy to implement, but due to inherent coupling effects between torque and flux that results in sluggish response and system being easily prone to instability, they do not produce satisfactory results for high performance applications. This problem can be addressed by applying direct torque control or field oriented control. In most control applications in industrial drives, the usual

approach to induction motor control involves the use of vector or field oriented control strategy so as to realize the best dynamic characteristics [1]. The use of this approach ensures decoupling between the flux and torque and thereby permits the control of induction motor in a similar way that separately excited direct current (DC) motors are controlled. Thus for high performance applications vector controlled induction motor can be employed [3].

The performance response of the speed of the induction motor was evaluated considering two conditions, which include when the PID controller was not in the closed loop and when the controller was in the closed loop [4]. The torque and speed performance of induction motor has been examined by [5] using simplified vector control scheme integrating PI and PID controllers. A PID controller for speed control of single phase induction motor employed in rotary force spinning apparatus has been implemented in [6]. Pulse width modulation (PWM) technique and universal bridge has been used in [7] to control the speed of induction motor. In order to control the maximum direct current link voltage of voltage source inverter, a PID control technique was implemented. [8] compared the performance of various control techniques for speed control of induction motor. The control schemes considered in the study are PI, PID and Fuzzy logic controller (FLC).

Proportional-integral (PI) and proportional-integral-derivative (PID) controllers, which are conventional control techniques have been used together with vector control methods over the years to improve the speed control performance of induction motors. Nevertheless, there are major drawbacks to the use of conventional controllers such as performance sensitivity to variations in system parameters. The PI and PID controllers use fixed gains, and this may not yield the desired speed performance under motor parameter variations and operating conditions. Thus, intelligent control involving the use of Fuzzy Logic Controller (FLC) has been used for the control of speed [9].

In this paper, a conventional control technique is combined with fuzzy logic controller to achieve better results in terms of performance response of induction motor by eliminating drawbacks associated with conventional controllers such as overshoot, cycling, and undershoot and steady state error common with FLC. Steady state error is the difference between the desired (or reference) value (input) and the actual value (output).

II. SYSTEM MODEL

This section presents the model of the proposed induction motor speed control system using FLC aided PID controller with vector control technique as shown in Figure 3.1. There are two inputs to the FLC, the speed error signal (E) and the rate of change in speed error (dE/dt). The speed error occurs when there is difference between the reference (or desired) speed, ω_{ref} and the actual (or response) speed, ω_{act} of induction motor.

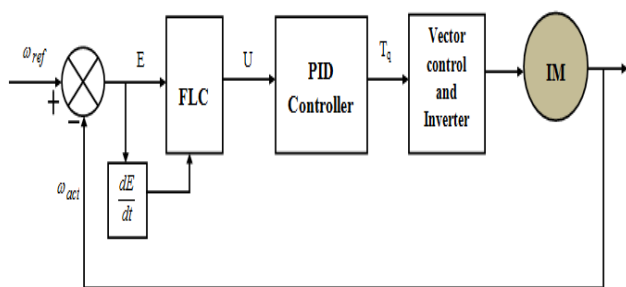


Fig. 1 Proposed system model

2.1 System Description

Figure 3.1 is the closed loop speed control system of the induction motor. The first input to the summing point is the set speed ω_{ref} , which is the reference or desired speed at which the induction motor is expected to run. The second input to the summing point is the feedback signal ω_{act} , which is the current speed of the induction motor detected or measured by a feedback mechanism. The deviation between these two inputs, called speed error signal, E and its derivative are fed to the FLC. The FLC then produces an appropriate output signal called control signal or command signal of FLC, U. The command

signal, U is fed to the PID controller and then used to optimize its parameters or gains. The resulting controller output T_q , which serves as the reference torque for indirect field oriented control is used to initialize the vector control and inverter mechanism, which produces a proportional output to rotate the induction motor so that its runs at speed according to the sign of the error signal and its derivative. Generally, the FLC-PID controller captures the speed error signal and correspondingly alters the current speed of the motor so that actual response speed of the induction motor matches the set speed.

2.2 Mathematical Model of Induction Motor

In this subsection, the dynamic equations that describe the characteristics of induction motor during operation are presented. In order to design a control system for electrical drives such as induction motor, the mathematical model is required. One requirement for any system that is to be control is that it should be represented in either state space form or as a transfer function. Hence, the transfer function of induction motor is required to design the controller. Thus, the equivalent circuit of induction motor in direct axis and quadrature axis (d-q axis) as shown in Figure 2 is employed in the dynamic modelling of the induction motor.

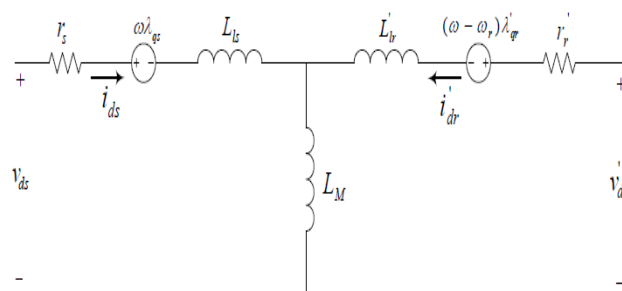


Fig. 2a. Equivalent circuit model of induction motor in d-axis frame [10]

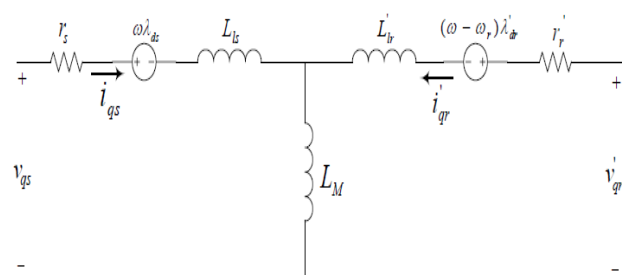


Fig2b. Equivalent circuit model of induction motor in q-axis frame [10]

Figure 2 shows the equivalent circuit for determining the dynamic equations that represent the model of induction motor. The concept of a rotating d-q field reference (without saturation) is used to develop induction motor model [4]. The voltage required to drive the flux and torque to the expected values within a given time period is calculated using induction motor model [4]. The dynamic model of the induction motor in Simulink is used to analyze the calculated voltage.

In deriving the mathematical equations representing the dynamic behaviour of the induction motor, it is necessary to make the assumption that the rotor bars are short circuited and there is no load [10]. It should be noted that all variables shown in Figure 2 and all through this mathematical formulation are referenced to the stator.

Modelling of induction motor in terms of d-q model begins with the Park Transformation of the 3-phase stationary reference variables a-b-c, which 120° apart into 2-phase stationary reference variables d-q. In addition, these 2-phase variables are transformed into synchronously rotating reference variables and vice versa. Assuming that d-q axes are tilting (or oriented) at an angle of θ , the direct axis voltage v_d and quadrature axis voltage v_q can be resolved into a-b-c component and then written in vector-matrix form as:

$$\begin{bmatrix} v_q \\ v_d \\ v_0 \end{bmatrix} = \frac{2}{3} \begin{bmatrix} \cos\theta & \cos(\theta - \gamma) & \cos(\theta - \gamma) \\ \sin\theta & \sin(\theta - \lambda) & \sin(\theta + \lambda) \\ 0.5 & 0.5 & 0.5 \end{bmatrix} \begin{bmatrix} v_a \\ v_b \\ v_c \end{bmatrix} \quad (1)$$

where v_0 is added as zero sequence element that may or may not be present. Also, v_a, v_b, v_c are the various voltages resolved into a-b-c component. Equation (1) can be simplified further as shown in Eq. (2) and (3) [10]:

$$v_{dq0} = [K_s][v_{abc}] \quad (2)$$

where,

$$v_{dq0} = \begin{bmatrix} v_q \\ v_d \\ v_0 \end{bmatrix}, \quad K_s = \frac{2}{3} \begin{bmatrix} \cos\theta & \cos(\theta - \gamma) & \cos(\theta - \gamma) \\ \sin\theta & \sin(\theta - \lambda) & \sin(\theta + \lambda) \\ 0.5 & 0.5 & 0.5 \end{bmatrix}, \quad v_{abc} = \begin{bmatrix} v_a \\ v_b \\ v_c \end{bmatrix} \quad (3)$$

The d-q model derivation is further presented in mathematical form, which is followed by a circuit analysis technique. In addition, the concept presented in [11] is considered in this work as follows using Figures 2 and 3:

$$v_{dq0s} = r_s i_{dq0s} + \omega \lambda_{dq0s} + p \lambda_{dq0s} \quad (4)$$

$$v_{dq0r} \lambda'_{dq0r} = r_r i'_{dq0r} + (\omega - \omega_r) \lambda'_{dq0r} + p \lambda'_{dq0r} \quad (5)$$

where v_{dq0s} is the d-q axis stator voltage, r_s is the stator resistance, i_{dq0s} is the d-q axis stator current, ω is the electrical speed, p is number of poles, λ_{dq0s} is the d-q axis flux linkage in the stator variable, v_{dq0r} is the d-q axis rotor voltage, λ'_{dq0r} is the is d-q axis flux linkage in

the rotor variable, r_r is the rotor resistance, i'_{dq0r} is the d-q axis rotor current, ω_r is the rotor electrical speed.

The d-q flux linkages in the stator and rotor variables are defined as given by [10]:

$$\begin{bmatrix} \lambda_{dq0s} \\ \lambda'_{dq0s} \end{bmatrix} = \begin{bmatrix} K_s L_s K_s^{-1} & K_s L_{sr} K_r^{-1} \\ K_r (L'_{sr})_T K_s^{-1} & K_r L_r K_r^{-1} \end{bmatrix} \begin{bmatrix} i_{da0s} \\ i'_{dq0r} \end{bmatrix} \quad (6)$$

$$K_s L_s K_s^{-1} = \begin{bmatrix} L_{Is} + L_M & 0 & 0 \\ 0 & L_{Is} + L_M & 0 \\ 0 & 0 & L_{Is} + L_M \end{bmatrix} \quad (7)$$

where $L_M = \frac{3}{2} L_m$

Similarly,

$$K_r L_r K_r^{-1} = \begin{bmatrix} L_{Ir} + L_M & 0 & 0 \\ 0 & L_{Ir} + L_M & 0 \\ 0 & 0 & L_{Ir} + L_M \end{bmatrix} \quad (8)$$

and

$$K_s L_{sr} K_r^{-1} = K_r (L'_{sr})_T K_s^{-1} = \begin{bmatrix} L_M & 0 & 0 \\ 0 & L_M & 0 \\ 0 & 0 & 0 \end{bmatrix} \quad (9)$$

Thus, the derivation of d-q flux formulae is determined from the following matrix [10]:

$$\begin{bmatrix} \lambda_{qs} \\ \lambda'_{qr} \\ \lambda_{ds} \\ \lambda'_{dr} \end{bmatrix} = \begin{bmatrix} L_{ss} & L_M & 0 & 0 \\ L_M & L_{rr} & 0 & 0 \\ 0 & 0 & L_{ss} & L_M \\ 0 & 0 & L_M & L_{rr} \end{bmatrix} \begin{bmatrix} i_{qs} \\ i'_{qr} \\ i_{ds} \\ i'_{dr} \end{bmatrix} \quad (10)$$

where $K_s L_s K_s^{-1}$, $K_r L_r K_r^{-1}$, and $K_s L_{sr} K_r^{-1}$ are the stator mutual inductance, rotor mutual inductance, and stator-rotor mutual inductance, L_{Is} is the stator inductance, L_{Ir} is the rotor inductance, L_m is the mutual winding inductance, λ_{ds} , λ_{qs} , λ'_{dr} and λ'_{qr} are the flux linkages for the stator d-axis/q-axis and the rotor d-axis/q-axis, i_{ds} , i_{qs} , i'_{dr} and i'_{qr} are the stator current for d-axis/q-axis and the rotor current for d-axis/q-axis respectively.

Now, further application is made using the equivalent circuit diagram in Figure 2 to carry out circuit analysis from the d-axis and q-axis circuits to determine the d-axis and q-axis stator and rotor voltages. It is again assumed that for the induction, the rotor bars are short circuited and thus rotor voltages, v_{dr} and v_{qr} are equal to zero [10].

Hence, the d-axis and q-axis voltages of the stator are given by:

$$v_{qs} = r_s i_{qs} + \omega \lambda_{ds} + p \lambda_{qs} \quad (11)$$

$$v_{ds} = r_s i_{qs} - \omega \lambda_{qs} + p \lambda_{ds} \quad (12)$$

The flux linkages given in Eq. (10) are further defined by the following equations:

$$\lambda_{qs} = L_{Is}i_{qs} + L_m(i_{qs} + i'_{qr}) \quad (13)$$

$$\lambda_{ds} = L_{Is}i_{ds} + L_m(i_{ds} + i'_{dr}) \quad (14)$$

$$\lambda'_{qr} = L'_{Ir}i'_{qr} + L_m(i_{qs} + i'_{dr}) \quad (15)$$

$$\lambda'_{dr} = L'_{Ir}i'_{dr} + L_m(i_{qs} + i'_{dr}) \quad (16)$$

It is important to transform the reluctance of the stator, the rotor, and the mutual winding to inductance so as to calculate the current and flux linkages. In order to achieve this transformation, the relationship between reluctance and inductance for alternating current circuit is employed as follows:

$$L_{Is} = \frac{X_s}{2\pi f} \quad (17)$$

$$L_{Ir} = \frac{X_r}{2\pi f} \quad (18)$$

In the same vein, the inductance of the mutual winding is given by:

$$L_m = \frac{2}{3} \frac{X_s}{2\pi f} \text{ or } L_m = \frac{X_s}{2\pi f} \quad (19)$$

Thus, the self-inductance of the stator and rotor are given by:

$$L_s = L_m + L_{Is} \quad (20)$$

$$L_r = L_m + L_{Ir} \quad (21)$$

Solving for d-axis/q-axis stator and rotor current as shown in Figure 2 in terms of flux linkages results in:

$$i_{ds} = \lambda_{ds} \frac{L_r}{L_s L_r - L_m^2} - \lambda'_{dr} \frac{L_r}{L_s L_r - L_m^2} \quad (22)$$

$$i_{qs} = \lambda_{qs} \frac{L_r}{L_s L_r - L_m^2} - \lambda'_{qr} \frac{L_r}{L_s L_r - L_m^2} \quad (23)$$

$$i'_{dr} = \lambda'_{dr} \frac{L_r}{L_s L_r - L_m^2} - \lambda_{ds} \frac{L_r}{L_s L_r - L_m^2} \quad (24)$$

$$i'_{qr} = \lambda'_{qr} \frac{L_r}{L_s L_r - L_m^2} - \lambda_{qs} \frac{L_r}{L_s L_r - L_m^2} \quad (25)$$

Rate of flux linkages of the stator and rotor in terms of d-axis and q-axis variable elements can be computed as follows:

$$\begin{aligned} \frac{d\lambda_{ds}}{dt} &= v_{ds} - \lambda_{ds} \frac{r_s L_r}{L_r L_s - L_m^2} \\ &+ \lambda'_{dr} \frac{r_s L_m}{L_r L_s - L_m^2} + \omega \lambda_{qs} \end{aligned} \quad (26)$$

$$\begin{aligned} \frac{d\lambda_{qs}}{dt} &= v_{qs} - \lambda_{ds} \frac{r_s L_r}{L_r L_s - L_m^2} \\ &+ \lambda'_{qr} \frac{r_s L_m}{L_r L_s - L_m^2} + \omega \lambda_{ds} \end{aligned} \quad (27)$$

$$\begin{aligned} \frac{d\lambda'_{dr}}{dt} &= 0 - \lambda'_{dr} \frac{r_r L_r}{L_r L_s - L_m^2} + \lambda_{ds} \frac{r_r L_m}{L_r L_s - L_m^2} \\ &+ (\omega - \omega_r) \lambda'_{qr} \end{aligned} \quad (28)$$

$$\begin{aligned} \frac{d\lambda'_{qr}}{dt} &= 0 - \lambda'_{qr} \frac{r_r L_r}{L_r L_s - L_m^2} + \lambda_{qs} \frac{r_r L_m}{L_r L_s - L_m^2} \\ &+ (\omega - \omega_r) \lambda'_{dr} \end{aligned} \quad (29)$$

Equation (29) completes the d-q modelling of induction motor. The implementation of d-q model induction motor will be carried out in MATLAB/Simulink environment. The electrical torque (T_e) of induction motor and rotor speed can be computed using the following equations [10]:

$$T_e = \frac{3pL_m}{4} (i_{qs}i'_{dr} - i_{ds}i'_{qr}) \quad (30)$$

$$\frac{d\omega_r}{dt} = \frac{T_e - B\omega_r}{J} \quad (31)$$

where B, J are the friction coefficient and rotor initial respectively. The Laplace transform of the rotor speed in Eq. (31) becomes:

$$\omega_r(s) = \frac{T_e}{Js + B} \quad (32)$$

Therefore, Eq. (32) is rotor speed dynamic characteristics of the induction motor.

III. CONTROLLER DESIGN

A Proportional Integral Derivative (PID) controller is a generic control loop feedback mechanism widely used in industrial control systems and regarded as the standard control structures. This is because it is simple and easy to implement [12], [13]. A PID controller, sometimes called three-term control, calculates an error value as the difference between a measured process variable and a desired setpoint. The controller attempts to minimize the error by adjusting the process through the use of a manipulated variable. The PID controller has the optimum control dynamics including zero steady state error, fast response (short rise time), no oscillations and higher stability. The necessity of using a derivative gain component in addition to the PI controller is to eliminate the overshoot and the oscillations occurring in the output response of the system. One of the main advantages of the PID controller is that it can be used with higher order processes including more than single energy storage. Figure 3 shows the control system schematic model with general PID controller.

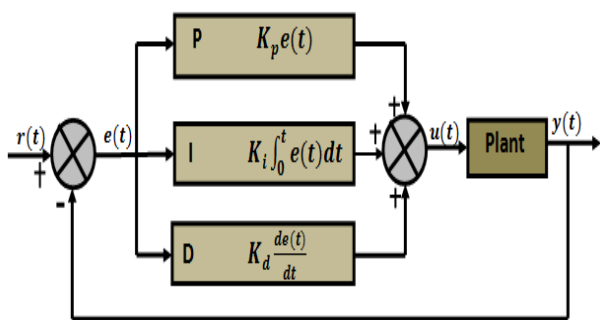


Fig. 3 Model of PID controller

In Figure 3, K_p = proportional gain, K_i = integral gain, and K_d = derivative gain. There are three separate constant parameters (Controller Gains) involved in PID control technique.

The overall mathematical description of linear relationship existing between the controller output, $u(t)$ and the error, $e(t)$ in Figure 3 is expressed as in Eq. (33).

$$u(t) = K_p e(t) + K_i \int e(t)dt + K_d \frac{d}{dt}e(t) \quad (33)$$

Applying the PID controller to any control system involves adjusting the values of gain K_p , K_i and K_d in order to get the best response of the system. The selection of PID controller gain values causes the variation of observed response with respect to desired response.

The developed PID controller with $K_p = 1.2$, $K_i = 0.1$, and $K_d = 0.2$ is given by:

$$Y(s) = \frac{U(s)}{E(s)} = 1.2 + \frac{0.1}{s} + 0.2s \quad (34)$$

The Simulink model of the implemented PID controller is shown in Fig. 4.

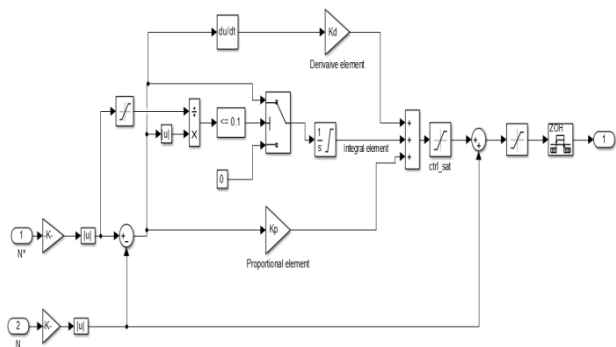


Fig. 4 Simulink model of implemented PID control technique

3.1 Design of Fuzzy Logic Controller

The design and implementation of FLC is carried out in MATLAB/Simulink environment using the Mamdani model and the method of defuzzification used is centre of gravity. With FLC usually characterised by at least two inputs and one output, mapping of inputs to output is done by Mamdani fuzzy inference system (FIS) using membership functions (MFs) of the fuzzy sets. A shape as shown in Figure 5, which shows the mode by which every point in the input crisp value is tied to a degree of fuzzy value is called membership function (MF) [14].

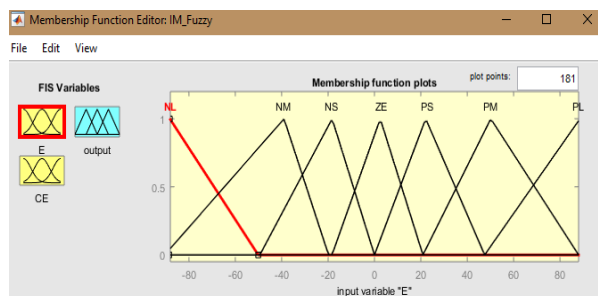


Fig. 5a. Error input (E) of fuzzy logic membership function

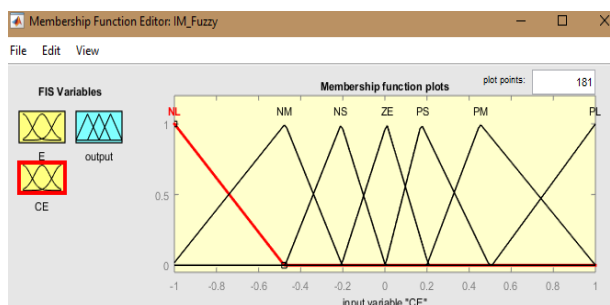


Fig. 5b Change error input (CE) of fuzzy logic membership function

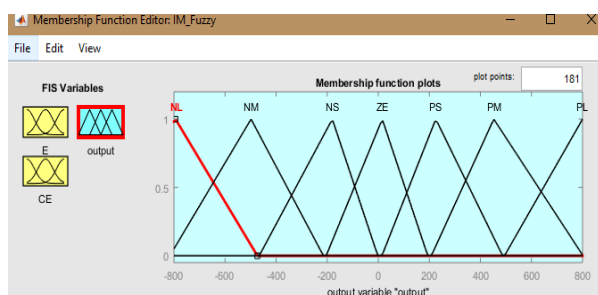


Fig. 5c Output variable of fuzzy logic membership function

In Figure 5, the inputs and outputs were modeled using triangular MF. A three-dimensional (3-D) graphical representation of the mapping of the inputs to the output called control surface [14] is presented in Figure 6. The rule viewer of the relationship and process of the E and CE producing an output is shown in Figure 7.

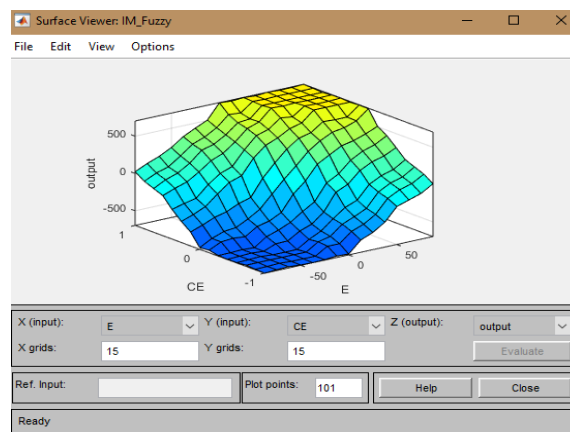


Fig. 6 Fuzzy logic control surface

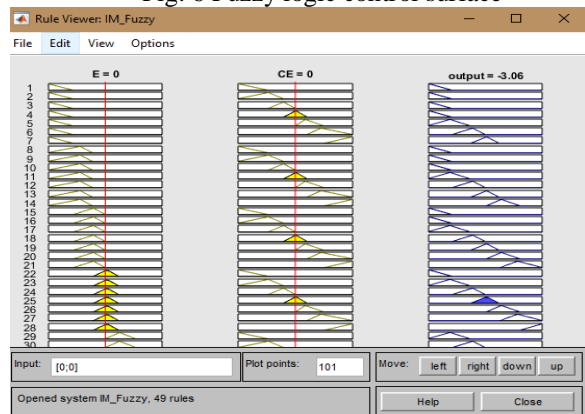


Fig. 7 Fuzzy logic control rule viewer

3.2 Simulation Parameters

The induction motor considered in this work is rated 1.5KW and its parameters are presented in Table 1.

Table 1 Rating of induction motor [10]

| Parameter | Unit | Rating |
|----------------------|-------------------|--------|
| Number of poles (p) | - | 4 |
| Power | kW | 1.5 |
| Current | A | 6.1 |
| Speed | rpm | 1725 |
| Stator resistance | Ω | 1.5 |
| Rotor resistance | Ω | 0.95 |
| Stator reluctance | Ω | 1.40 |
| Rotor reluctance | Ω | 1.40 |
| Rotor inertial | Kg/m ² | 0.0138 |
| Friction coefficient | Nm.s/rad | 0.0031 |
| Frequency | Hz | 50 |

IV. SIMULATION RESULT

This section presents the simulation results obtained from the MATLAB/Simulink simulation analysis of the proposed system. A step forcing input of magnitude 1725 representing the rated or desired speed of the induction motor (1725 rpm) was applied at the input in order to study the ability of the induction motor to run at the rated speed. Simulations were carried out considering four tests in terms of step response of actual speed of the induction motor when the designed Fuzzy-PID controller has not been added to the control (that is system without controller), step response speed of the system at no load torque effect with designed Fuzzy-PID controller, step response speed under load torque with Fuzzy-PID controller, and finally the step response performance comparison of Fuzzy-PID control induction motor and conventional PID control induction motor. The performance of the closed loop control system is presented in terms of transient and steady state time domain step response parameters, namely: rise time, peak time, peak overshoot, settling time, final value and steady state error.

4.1 Step Response of Induction Motor without Fuzzy-PID Controller

The initial performance of the developed induction motor speed control system was tested based on simulation conducted in MATLAB/Simulink environment considering when the system is operating without the introduction of the developed Fuzzy-PID controller into the closed loop. The step response plot of the actual speed with respect to the rated or desired speed of the motor is shown in Figure 8. The steady state and transient performance characteristics of the actual response speed are stated in Table 2 with their respective values.

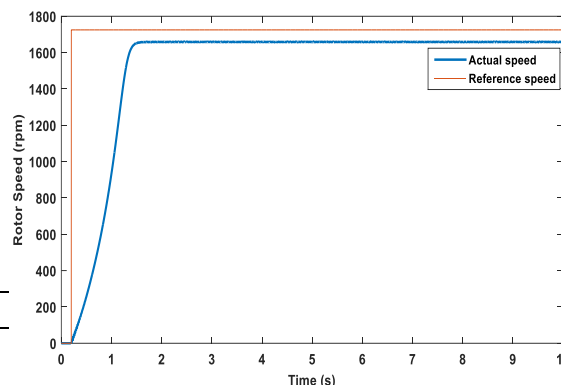


Fig. 8 Actual speed of induction motor (without a controller)

Table 2 Step response parameter without controller

| Parameter | System Performance |
|--------------------|--------------------|
| Rise time | 0.8685 s |
| Peak time | 3.2475 s |
| overshoot | 0.0469 % |
| Settling time | 1.3993 s |
| Final value | 1659 rpm |
| Steady state error | 66 rpm |

Looking at Figure 8 and Table 2, it can be seen that the expected rated speed at which the induction motor is expected or required to run is not achieved or reached by the system in this uncompensated state. That is at this state without a controller. Thus, there is need for a strategy that will ensure that the motor run at the rated speed. Though the time domain performance parameters such as rise time of 0.8685 seconds, peak time of 3.2475 seconds, peak overshoot of 0.0469% and settling time of 1.3993 seconds seemed promising, the steady state value was 1659 rpm and represents the actual speed at which the motor is running. The difference between the rated or desired speed and the actual response speed is the steady state error is 66 rpm.

4.2 Step Response of Induction Motor with Fuzzy-PID Controller

In this subsection, the simulation results achieved by incorporating a Fuzzy-PID controller considering zero load torque and under load torque are presented as shown in Figure 9 and Figure 10 respectively. The numerical

analysis of the transient and steady state performance time domain parameters from each simulation plots are shown in Table 3.

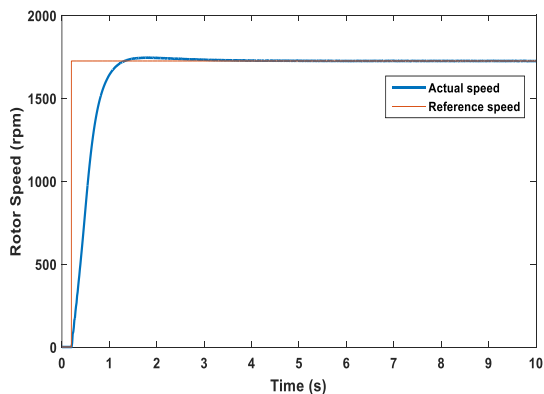


Fig. 9 Actual speed of induction motor with Fuzzy-PID (at zero torque)

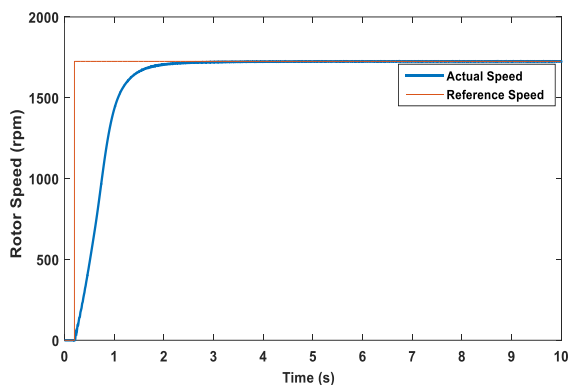


Fig. 10 Actual speed of induction motor with Fuzzy-PID (under load torque)

Table 3 Step response parameter with Fuzzy-PID controller

| Parameter | System Performance | |
|--------------------|--------------------|-------------------|
| | Zero torque | Under load torque |
| Rise time | 0.5878 s | 0.8354 s |
| Peak time | 1.7675 s | 4.9615 s |
| overshoot | 1.1582 % | 0.0352 % |
| Settling time | 1.1355 s | 1.2240 s |
| Final value | 1745.1 rpm | 1724.9 rpm |
| Steady state error | 20.1 rpm | 0.1 rpm |

From Figures 9 and 10, it can be seen that the addition of Fuzzy-PID controller into the closed loop control system of the induction motor largely improved the actual speed response performance. Table 3 shows the numerical performance analysis of each simulation condition involving the introduction of Fuzzy-PID controller at zero load torque and at unit load torque. It is obvious that the system at zero load torque provided better performance in terms of rise time (0.5878 seconds), peak time (1.7675 seconds) and settling time (1.1355 seconds) compared with the system subject to unit load of rise time (0.8354 seconds), peak time (4.9615 seconds) and settling time (1.2240 seconds). However, in terms of peak overshoot, steady state value and steady state error, the unit load

torque system offered better performance result with values of 0.0352 %, 1724.9 rpm and 0.1 rpm against 1.1582 %, 1745.1 rpm and 20.1 rpm for no load torque condition. Generally, considering the time domain performance parameters in both cases, it can be said that the system provided improved and promising performance. Nevertheless, at no load torque the steady state speed or actual speed of the motor was somewhat slightly higher than rated or desired speed at which the motor is required to run and therefore resulting in steady state error of 20.1 rpm. Then with addition of load torque, the system seems to be better stabilized considering an overshoot of 0.0352% and achieve the desired or rated motor torque with negligible steady state error of 0.1 rpm. This conforms to a practical scenario where an induction motor is normally expected to run at the rated speed under load torque.

4.3 Performance Comparison of Fuzzy-PID and Conventional PID

In order to validate the superiority of the proposed intelligent aided conventional PID controller (Fuzzy-PID controller) over the conventional PID controller, simulation was conducted considering both PID controller and Fuzzy-PID controller compensated closed loop control system for induction motor under load torque. The simulation result of the system in both cases subject to step input of magnitude 1725 rpm of the rated speed is shown in Fig. 11. The numerical performances of the plots are shown in Table 4.

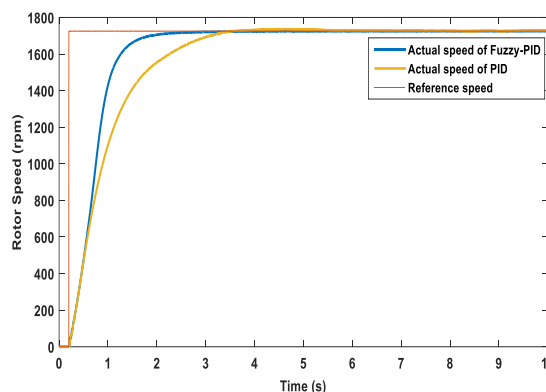


Fig. 11. Performance comparison plots (PID and Fuzzy-PID)

Table 4 Comparison of step response performance parameters

| Parameter | System Performance | |
|--------------------|--------------------|------------|
| | PID | Fuzzy-PID |
| Rise time | 1.6723 s | 0.8354 s |
| Peak time | 4.5475 s | 4.9615 s |
| Peak overshoot | 0.6913 % | 0.0352 % |
| Settling time | 2.9646 s | 1.2240 s |
| Final value | 1736.1 rpm | 1724.9 rpm |
| Steady state error | 11.1 rpm | 0.1 rpm |

Looking at Table 4, it can be deduced that the Fuzzy-PID control induction motor outperformed the conventional

PID control system for all time domain transient and steady state response parameters except for the peak time. This will have no effect since the system with Fuzzy-PID controller must reached the rated speed and stabilized before the PID controller will even reached the peak time. The Fuzzy-PID controller provided robust, fast and perfect tracking of desired speed and maintained this speed with negligible peak overshoot of 0.0352% and steady state error 0.1 rpm.

V. CONCLUSION

An intelligent aided conventional PID controller has been implemented as an element of closed loop speed control system for induction motor. The intelligent algorithm used was that of fuzzy logic. The dynamic equations of an induction motor were determined and modelled in MATLAB/Simulink. Simulation was conducted using the parameters of an induction motor of rated power 1.5 kW and speed of 1725 rpm. The performance of the closed loop control system was initially examined in absence of a controller. This was performed in order to understand the speed performance of the induction motor when operated without a technique to compensate its transient and steady state time domain performance parameters. Simulation result showed that the induction motor in this condition was not able run at the rated speed. Thus, there was need for a technique to compensate for this inadequacy. A Fuzzy-PID control scheme was developed in MATLAB/Simulink and then added to the closed loop speed control of induction motor. With the Fuzzy-PID controller, two simulation scenarios were considered, which are: no load torque and under load torque. The Fuzzy-PID control system under load torque yield better performance than the case with no load torque. Furthermore, the superiority of the proposed scheme over conventional PID was examined. The results obtained revealed the superiority of Fuzzy-PID over PID.

REFERENCES

- [1] A. Fattah, "Design and analysis of speed control using hybrid PID-Fuzzy controller for induction motors," Master's Thesis, Western Michigan University, 2015.
- [2] A. Kusagur, S. F. Kodad, & S. Ram, "Modelling & simulation of an ANFIS controller for an AC drive," *World Journal of Modelling and Simulation*, vol. 8, No. 1, pp. 36-49, 2011.
- [3] P. K. Behera, M. K. Behera, & A. K. Sahoo, "Comparative analysis of scalar & vector control of induction motor through modeling & simulation," *International Journal of Innovative Research in Electrical, Electronics, Instrumentation and Control Engineering*, vol. 2, No. 4, pp. 1340-1344, 2014.
- [4] A. A. Idoko, I. T. Thuku, S. Y. Musa, & C. Amos, "Design of tuning mechanism of PID controller for application in three phase induction motor speed control," *Int. Journal of Advanced Engg Research & Science*, vol. 4, No. 11, pp. 138 – 146, 2017.
- [5] D. T. Korsane, A. Polke, S. K. Mude, C. S. Hiwarkar, K. Korsane, "Speed performance of three phase induction motor by using simplified vector control method," *International Journal of Engineering Research in Electrical and Electronic Engineering*, vol. 4, No. 3, pp. 172 – 178, 2018.
- [6] Y. Sanjaya, A. Fauzi, D. Edikresnha, M. M. Munir, M. M., & Khairurijal, "Single phase induction motor speed regulation using a PID controller for rotary forcespinning apparatus," *Procedia Engineering*, vol. 170, pp. 404 – 409, 2017.
- [7] H. Hartono, R. I. Sudjoko, & P. Iswahyudi, "Speed control of three phase induction motor using universal bridge and PID controller," *Journal of Physics: Conference Series*, 1381, 012053, 2019.
- [8] Irianto, F. D. Murdianto, E. Sunarno, & D. D. Proboningtyas, "Comparison method of PI, PID, and fuzzy logic controller to maintain speed stability in single phase induction motors," *INTEK Jurnal Penelitian*, vol. 8, No.1, pp. 7 – 16, 2021.
- [9] C. Chengaiah, & S. Prasad, "Performance of induction motor drive by indirect vector controlled method using PI and fuzzy controllers," *International Journal of Science and Environment*, vol. 2, No. 3, pp. 475 – 469, 2013.
- [10] M. M. Malatji, "Derivation and implementation of a DQ model of an induction machine using MATLAB/Simulink," *Electromechanical Conversion*, Technical Report, pp. 1-8.
- [11] A. W. Leedy, "Simulink/MATLAB dynamic induction motor model for use in undergraduate electric machines and power electronics courses," 2013 *Proceedings of IEEE Southeast Conference*, Jacksonville, FL, 1-6.
- [12] P. O. Ugochukwu, P. C. Eze, & D. C. Oyiogu, "Enhance the performance of AVR system with prefilter aided PID controller," *Access International Journal of Research & Devel*, vol. 1, No. 1, pp. 21-32.
- [13] P. C. Eze, A. E., Jonathan, B. C. Agwah, & E. A. Okoronkwo, "Improving the performance response of mobile satellite dish antenna network within Nigeria," *Journal of Electrical Engineering, Electronics, Control and Computer Science*, vol. 6, No. 21, 25-30, 2020.
- [14] P. C. Eze, B. O. Ekengwu, N. C. Asiegbu, & T. I. Ozue, "Adjustable gain enhanced fuzzy logic controller for optimal wheel slip ratio tracking in hard braking control system," *Advances in Electrical and Electronic Engineering*, vol. 19, No. 3, pp. 231 – 242, 2021.